Journal of Alloys and Compounds 509 (2011) 15–20

Contents lists available at ScienceDirect

Journal of Alloys and Compounds

journal homepage: www.elsevier.com/locate/jallcom

Mechanochemical synthesis of nanocrystalline $ZnWO_4$ at room temperature

M. Mancheva[a,*], R. Iordanova[a,1], Y. Dimitriev[b]

[a] Institute of General and Inorganic Chemistry, Bulgarian Academy of Science, “Acad. G. Bonchev” str., bl.11, Sofia 1113, Bulgaria
[b] University of Chemical Technology and Metallurgy, 1756 Sofia, Bulgaria

ARTICLE INFO

Article history:
Received 26 May 2010
Received in revised form 29 July 2010
Accepted 8 August 2010
Available online 18 August 2010

Keywords:
$ZnWO_4$
Mechochemical reaction
Nanoparticles
Photocatalytic activity

ABSTRACT

Single nanocrystalline $ZnWO_4$ powders were successfully synthesized by ball milling at room temperature. A stoichiometric mixture of ZnO and WO_3 in a 1:1 molar ratio was subjected to intense mechanical treatment in air using a planetary ball mill (Fritsch – Premium line – Pulversette No. 7) for a period varying from 5 to 300 min. The influence of the four different milling conditions was investigated on the formation of $ZnWO_4$. The products obtained were characterized by X-ray diffraction (XRD), transmission electron microscopy (TEM), Brunauer–Emmer–Teller (BET) surface area, infrared (IR) spectroscopy and X-ray photoelectron spectroscopy (XPS). The synthesis of $ZnWO_4$ powder started after 5 min milling time and finished after 30 min milling time at a higher speed (1000 rpm). The mechanical treatment up to 300 min did not lead to phase and structure change of $ZnWO_4$. The product obtained contained nanoparticles with a size of about 50 nm. The photocatalytic activity of the $ZnWO_4$ powders obtained was investigated by degradation of a model aqueous solution of Malachite Green (MG) upon UV-light irradiation.

1. Introduction

$ZnWO_4$ belongs to the AWO_4 (A = Fe, Ni, Mn, Cd, Mg) group with wolframite type structure [1–3]. $ZnWO_4$ finds application as scintillator [4], magnetic and luminescent materials [5–14], gas-sensing [15–17] and a photocatalyst [18–30]. The properties of $ZnWO_4$ are closely related to crystallinity, particle size distribution and morphology and depend on the method of synthesis. Several approaches to the preparation of $ZnWO_4$ are reported in the literature: sol–gel [6,15–17], spray pyrolysis [7], low temperature methods [4,14,18,19], flux growth method [12,13], hydrothermal route [8,9,20–27], self-propagating combustion method [28], microwave-assisted solvothermal process [29], powerful ultrasonic irradiation method [30], solid state synthesis [31], polymerized complex method [32], molten salt method [33], solid state metathetic approach [34] and mechanochemical synthesis [35,36]. Pullar et al. used mechanochemical milling as a stage of standard ceramics mixed-oxide route [35]. For the synthesis of $ZnWO_4$ Dodd et al. [36] applied a 6 h mechanochemical treatment between H_2WO_4, $ZnCl_2$, Na_2CO_3 and NaCl followed by heat-treatment at 500 °C for 1 h and washing. Mechanochemical activation is well known method for the synthesis of advanced materials. This method is an effective, useful and simple to produce of nanocrystalline powders. Different mechanical routes for obtaining alloys, complex oxides, amorphous materials, catalysts, etc. have been developed [37–42]. There are many review connect with mechanochemical synthesis [43–45]. The many factors as milling speed, time of activation, diameter of balls, balls to powder weight ratio influence on the mechanochemical synthesis. Our previous results showed that mechanochemical treatment of NiO and MoO_3 and NiO and WO_3 led to direct synthesis of $NiMoO_4$ and $NiWO_4$ at room temperature [46,47]. This motivated us to continue to use pure oxides during mechanochemical treatment for the synthesis of compounds from the same groups as AWO_4. The purpose of the present work is to obtain nanocrystalline $ZnWO_4$ powders by mechanochemical activation of pure oxides (ZnO and WO_3) applying different experimental conditions: milling speed, ball milling time and diameters of balls.

2. Experimental

A stoichiometric mixture of ZnO (Merck, purity 99.9%) and WO_3 (Merck, purity 99.9%) in a 1:1 molar ratio was subjected to intense mechanical treatment at different periods of time (5–300 min) in air using a planetary ball mill (Fritsch – Premium line – Pulversette No. 7). Both vials and balls were of stainless steel. The balls to powder weight ratio was 10:1 which was established as appropriate in our previous studies [46,47]. The synthesis of $ZnWO_4$ was carried out at four different milling conditions varying in milling speed and balls diameter:

(i) milling speed of 500 rpm with balls of 5 mm in diameter;
(ii) milling speed of 850 rpm with balls of 5 mm in diameter;
(iii) milling speed of 850 rpm with balls of 10 mm in diameter;
(iv) milling speed of 1000 rpm with balls of 5 mm in diameter.

---

[*] Corresponding author. Tel.: +359 2 979 35 88; fax: +359 2 870 50 24.
E-mail address: mancheva@svr.igic.bas.bg (M. Mancheva).
[1] Tel.: +359 2 979 35 88; fax: +359 2 870 50 24.

0925-8388/$ – see front matter © 2010 Elsevier B.V. All rights reserved.
doi:10.1016/j.jallcom.2010.08.033

Table 1
The degree of phase transformations depending on milling speed at constant of diameter balls and milling time.

Starting materials/molar ratio	Vial/ball materials	The balls to powder weight ratio	Milling speed (rpm)	Diameter of balls (mm)	Milling time (min)	Present phases and vol % determined by "PowderCell" program
$ZnO:WO_3$ (1:1)	Stainless steel	10:1	500	5	5	ZnO (22%), WO_3 (78%);
					30	ZnO (10%), WO_3 (90%);
					120	$ZnWO_4$ (51.3%), ZnO (18.5%), WO_3 (30.2%);
					300	$ZnWO_4$ (100%);
$ZnO:WO_3$ (1:1)	Stainless steel	10:1	850	5	5	$ZnWO_4$ (12%), WO_3 (69%), ZnO (19%);
					30	$ZnWO_4$ (82%), WO_3 (14%), ZnO (4%);
					60	$ZnWO_4$ (100%);
					120	$ZnWO_4$ (100%);
					300	$ZnWO_4$ (100%);
$ZnO:WO_3$ (1:1)	Stainless steel	10:1	1000	5	5	$ZnWO_4$ (39%), WO_3 (47%), ZnO (14%);
					30	$ZnWO_4$ (100%);
					60	$ZnWO_4$ (100%);
					120	$ZnWO_4$ (100%);
					300	$ZnWO_4$ (100%);

The phase and structural transformations were monitored by X-ray diffraction (XRD) and infrared spectroscopy (IR). Powder XRD patterns were registered with a Bruker D8 Advance diffractometer using Cu K_α radiation in the range from 10 to 80°. The X-ray diffraction data were analyzed using the "PowderCell" program to determine the volume percentage of the phases present in the samples and to estimate the average crystallite size of $ZnWO_4$ [48]. The average crystallite size (D) resulting from X-ray diffraction broadening was also determined using the Scherrer formula at a peak $2\Theta = 18.90°$. The specific surface areas were measured by the Brunauer–Emmer–Teller (BET) method. Morphologies and crystallite sizes of the samples obtained were characterized by transmission electron microscopy—TEM (JOEL-100B). Infrared spectra were registered in the range 1200–400 cm^{-1} on a Nicolet-320 FTIR spectrometer using the KBr pellet technique. The XPS measurements were carried out in the UHV chamber of an ESCALAB-MkII (VG Scientific) electron spectrometer using MgK_α excitation with a total instrumental resolution of ~1 eV. Energy calibration was performed, taking the C 1s line at 285 eV as a reference. The photocatalytic activities of the $ZnWO_4$ powders obtained were evaluated by degradation of a model aqueous solution of Malachite Green (MG) upon UV-light irradiation. A Malachite Green (MG) solution (150 mL, 5 ppm) containing 0.1 g of as-prepared powder was placed in a glass beaker. Before the light was turned on, the solution was first ultrasonicated for 10 min and then stirred for 10 min to ensure equilibrium between the powders and the solution. Volumes of 3 mL solution were taken at given time intervals and separated through centrifugation (5000 rpm, 5 min). Then the concentration of MG in the solution was investigated with a Jenway 6400 spectrophotometer.

3. Results and discussion

3.1. XRD analysis

The X-ray diffraction patterns of the samples obtained by the different mechanochemical conditions are present in Fig. 1A–D. The diffraction lines of WO_3, ZnO and $ZnWO_4$ were indexed using JCPDS database. Tables 1 and 2 contain the present phases and vol.% determined by "PowderCell" program of the samples obtained by the different milling conditions. At the same time of mechanochemical activation (5, 30 and 60 min) and at the same diameters of the used balls (5 mm) with increasing of the milling speed the amount of the obtained $ZnWO_4$ increases (Table 1). At a 500 rpm milling speed the interaction between the initial oxides starts after 120 min milling time and completes after 300 min milling time (Table 1 and Fig. 1A). At 1000 rpm milling speed the chemical reaction starts after 5 min and finishes after 30 min milling time (Table 1 and Fig. 1D). For the same time of mechanochemical treatment (5, 30 and 60 min) and at the same milling speed (850 rpm) with increasing the diameters of the balls the amount of the synthesized $ZnWO_4$

Table 2
The degree of phase transformations depending on diameter of balls at constant of milling speed and milling time.

Starting materials/molar ratio	Vial/ball materials	The balls to powder weight ratio	Milling speed (rpm)	Diameter of balls (mm)	Milling time (min)	Present phases and vol.% determined by "PowderCell" program
$ZnO:WO_3$ (1:1)	Stainless steel	10:1	850	5	5	$ZnWO_4$ (12%), WO_3 (69%), ZnO (19%);
					30	$ZnWO_4$ (82%), WO_3 (14%), ZnO (4%);
						$ZnWO_4$ (100%);
					60	$ZnWO_4$ (100%);
					120	$ZnWO_4$ (100%);
					300	$ZnWO_4$ (100%);
$ZnO:WO_3$ (1:1)	Stainless steel	10:1	850	10	5	$ZnWO_4$ (26%), WO_3 (60%), ZnO (13%);
					30	$ZnWO_4$ (90%), WO_3 (10%);
					60	$ZnWO_4$ (100%);
					120	$ZnWO_4$ (100%);
					300	$ZnWO_4$ (100%);

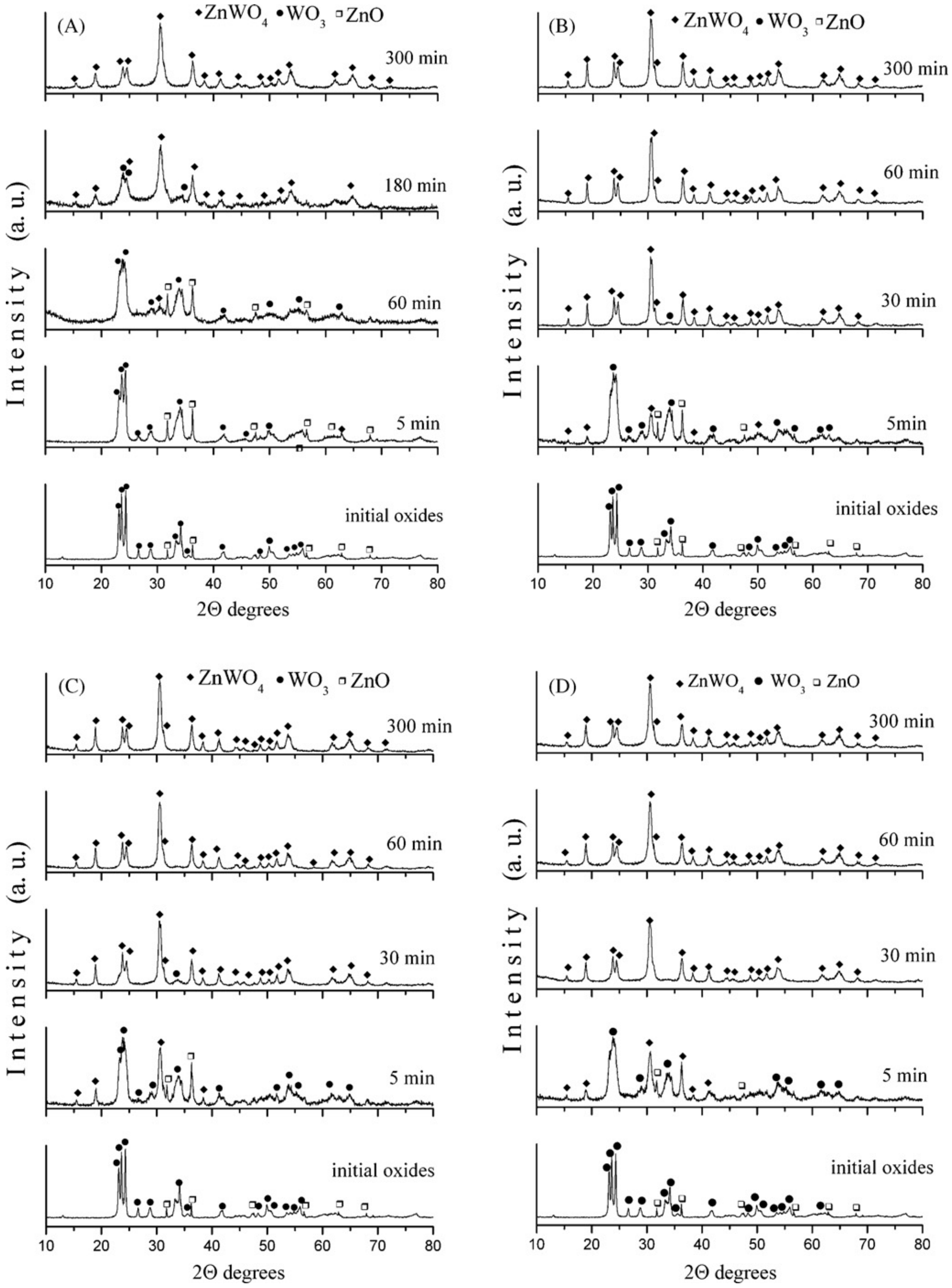

Fig. 1. (A) XRD patterns of the sample obtained at milling speed of 500 rpm with balls of 5 mm in diameter. (B) XRD patterns of the sample obtained at milling speed of 850 rpm with balls of 5 mm in diameter. (C) XRD patterns of the sample obtained at milling speed of 850 rpm with balls of 10 mm in diameter. (D) XRD patterns of the sample obtained at milling speed of 1000 rpm with balls of 5 mm in diameter.

increases (Table 2). Prolongation of mechanochemical treatment up to 300 min at milling speeds of 850 and 1000 rpm does not lead to a change in the XRD patterns of the samples. This is an indication of the structural stability of $ZnWO_4$. The obtained results show that the milling speed is decisive for the rapid synthesis. For comparison with published data $ZnWO_4$ was synthesized by a standard ceramics mixed-oxide route including milling at a lower milling speed (300 rpm) in water and calcination between 900 and 1200 °C [35]. A. Dodd et al. [36] applied a three stage process for the synthesis of $ZnWO_4$ consisting of mechanical milling (H_2WO_4, $ZnCl_2$, Na_2CO_3 and NaCl), low temperature heat-treatment and washing.

The BET surface area of the $ZnWO_4$ powder obtained at a milling speed of 1000 rpm (with balls of 5 mm in diameter) after 30 min milling time is 22 m^2/g. The surface area value is similar to the surface area of $ZnWO_4$ obtained by hydrothermal and low temperature methods [17,22–25,30]. The surface area decreases to 12 m^2/g after 300 min milling time. This fact may be due to some aggregation of the particles during mechanochemical treatment and that phase transformation of $ZnWO_4$ do not observed. The crystallite size estimated from the XRD peak at $2\Theta = 18.90^\circ$ using the Scherrer equation is 30 nm. The average crystallites sizes of $ZnWO_4$ calculated by the "PowderCell" program are in the range of 18 nm.

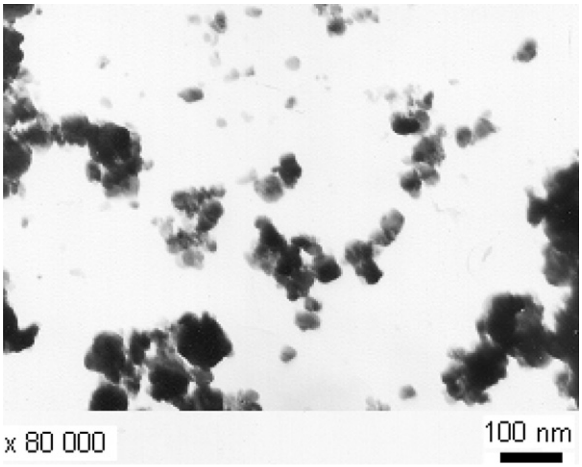

Fig. 2. TEM image of $ZnWO_4$ obtained at milling speed of 1000 rpm after 30 min milling time.

3.2. TEM analysis

The morphology and particle size of $ZnWO_4$ powders prepared after 30 and 300 min milling time at 1000 rpm milling speed are shown in Figs. 2 and 3, respectively. The TEM images show an irregular shape of the particles with size of about 50 nm. This size of the particles is in good agreement with the value determined by Scherrer equation (30 nm). At the selected milling conditions the dimension of aggregates is about 100 nm. After 300 min milling time the process of aggregation increases (dimension of aggregates reach 500 nm) which is in an agreement with the smaller value of the surface area.

3.3. Infrared analysis

IR spectroscopy was used to confirm the synthesis of the crystalline material. Fig. 4 presents the IR spectra of the sample obtained at 1000 rpm milling speed as a function of milling time. The absorption bands of the non-activated mixture of WO_3 (bands at 950, 820 and 760 cm^{-1}) and of ZnO (band at 420 cm^{-1}) [49–52] are shown in Fig. 4a. The observed new absorption bands at 870, 530 and 470 cm^{-1} evidences the beginning of the synthesis of $ZnWO_4$ after 5 min milling time (Fig. 4b). The noticeable changes in the IR spectrum were observed after 30 min milling time which are indication for the formation of $ZnWO_4$: shifting of the band at 820–840 cm^{-1}; increasing intensity of the bands at 870 and 840 cm^{-1}; appearance of the new bands below 700 cm^{-1} (Fig. 4c). In the wolframite type structure AWO_4 (A = Fe, Ni, Mn, Cd, Mg, Zn) the main structural units are W_2O_8 (formed by edge shared WO_6 groups) with two short bonds WO_2. As a result of edge shared octahedra W_2O_2 units arise [1–3]. The vibrational spectrum of $CdWO_4$ has been analyzed using Factor group analysis and the correlation method [53]. Fomichev and Kondratov performed theoretical group analysis of several compounds with wolframite structure [54]. Taking into account structural data and vibrational spectra of these compounds, we attributed the vibrational bands of the $ZnWO_4$. The bands at 870 and 840 cm^{-1} are due to vibration of the WO_2 entity present in the W_2O_8 groups. The bands at 685 and 650 cm^{-1} are typical of a two-oxygen bridge (W_2O_2) and are due to the asymmetric stretching of the same units [47,53,54]. The vibrations of the ZnO_6 polyhedra are in the absorption range below 600 cm^{-1} [47,53,54]. The band position and the band intensity do not change after prolonged milling times which confirm structural stability of $ZnWO_4$ (Fig. 4d and e).

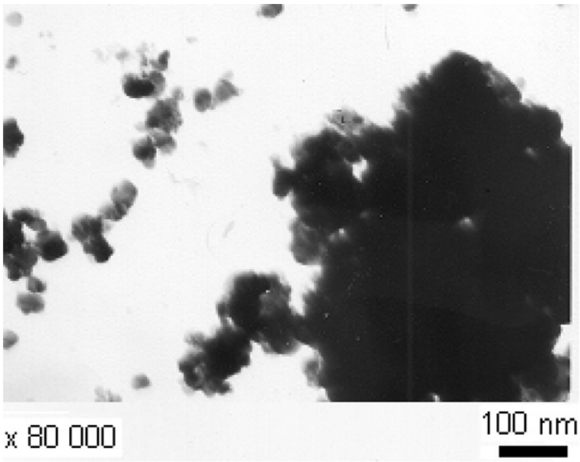

Fig. 3. TEM image of $ZnWO_4$ obtained at milling speed of 1000 rpm after 300 min milling time.

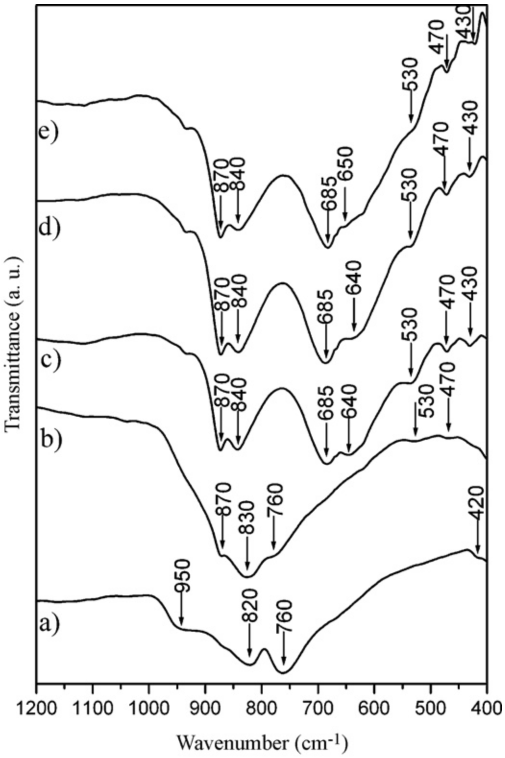

Fig. 4. IR spectra of sample: (a) before ball milling; (b) after 5 min ball milling; (c) after 30 min ball milling; (d) after 60 min ball milling; (e) after 300 min ball milling.

3.4. XPS analysis

XPS was performed to determine the oxidation state of Zn and W ions in the synthesized $ZnWO_4$. The XP spectra of Zn $2p_{3/2}$, W $4f_{7/2}$ and O 1s levers are presented in Fig. 5a–c respectively. The binding energy of the main Zn $2p_{3/2}$ line is at 1022 eV and is typical of the Zn^{2+} oxidation state in mixed oxides which is in good agreement with published data [16,29,30,34,55]. The W4f line is slightly broadened and presented by two components with binding energies of W $4f_{7/2}$ at 36.3 and at 34.8 eV, respectively (Fig. 5b). The higher binding energy value (36.3 eV) can be attributed to the W^{6+} oxidation state [16,29,30,34,56], while the lower value (34.8 eV) may be assigned to the W^{5+} oxidation state [16,29,30,34,56]. The amount of W^{5+} ions is about 7%. Similar results were obtained in our previous paper for $NiWO_4$ also synthesized by mechanochemical treatment

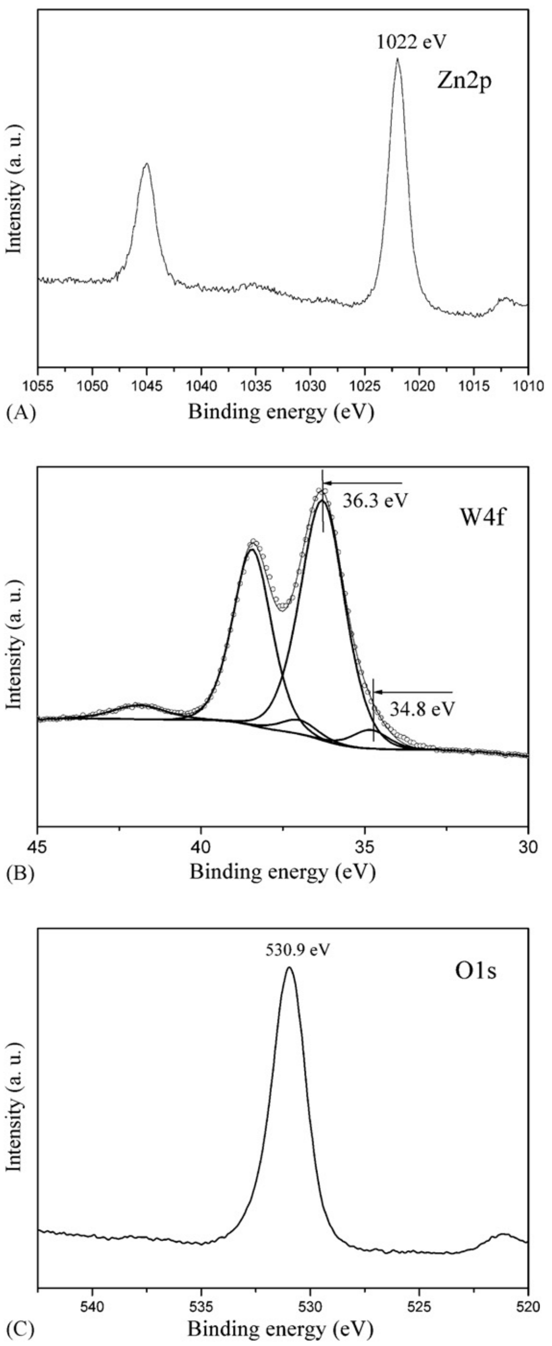

Fig. 5. X-ray photoelectron spectra of the $ZnWO_4$ obtained at milling speed of 1000 rpm after 30 min milling time: (a) of the Zn 2p level; (b) of the W4f level; (c) of the O 1s level.

[47]. This fact is probably due to the formation of a defect structure of $ZnWO_4$ during ball milling or partially to insignificant reduction during the XPS analysis. The O 1s line is symmetric and shows a sharp peak centered around 530.9 eV (Fig. 5c) [16,29,30,34].

3.5. Photocatalytic activity

The photodegradation of MG was tested as a model reaction to evaluate the photocatalytic activity of the $ZnWO_4$ powders obtained by different mechanochemical conditions. The sample obtained at a milling speed of 1000 rpm (sample D) exhibit higher photocatalytic activity in the degradation of MG as compared to other samples (Fig. 6). For example at 150 min irradiation time the degree of degradation of MG is 0.6 for the sample D (obtained at a milling speed of 1000 rpm), while the degrees of degradation of MG is 0.15 for the sample A (obtained at a milling speed of 500 rpm). The observed aggregation of the nanoparticles during mechanochemical treatment is probably the reason for the lower photocatalytic activity as compared to data of Lin et al. [25] for nanorod $ZnWO_4$ powders. $ZnWO_4$ powder was filtered and characterized by IR spectroscopy after the photocatalytic reaction. There is no change in the bands position (Fig. 7). This evidences that $ZnWO_4$ is stable during the photocatalytic test.

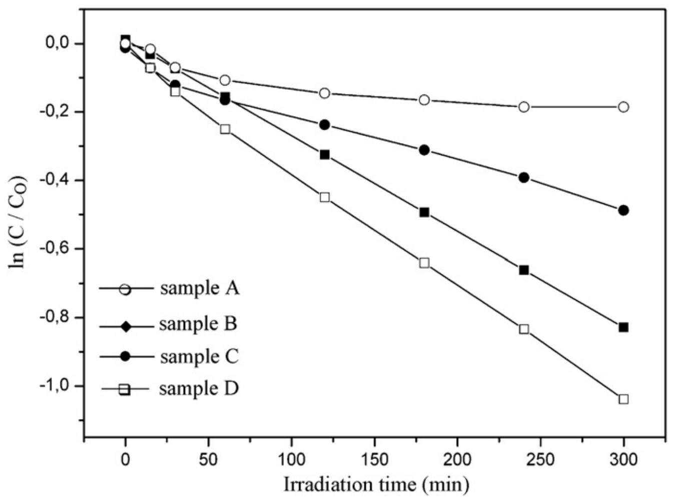

Fig. 6. Decomposition of the MG during UV-light irradiation by $ZnWO_4$ powders: sample A obtained at milling speed of 500 rpm with balls of 5 mm in diameter; sample B obtained at milling speed of 850 rpm with balls of 5 mm in diameter; sample C obtained at milling speed of 850 rpm with balls of 10 mm in diameter; sample D obtained at milling speed of 1000 rpm with balls of 5 mm in diameter.

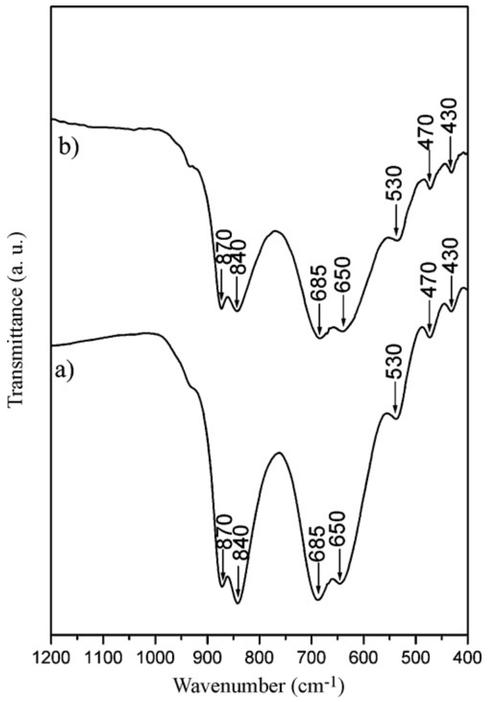

Fig. 7. IR spectra of $ZnWO_4$ powder: (a) before photocatalytic test and (b) after photocatalytic test.

4. Conclusions

The influence of the mechanochemical conditions: milling speed, milling time and diameters of the used balls on the formation of $ZnWO_4$ has been established. It is found that milling speed is decisive factor for the rapid synthesis. The best results are obtained at milling speed of 1000 rpm with balls of 5 mm in diameter and 30 min milling time. The obtained nanocrystalline $ZnWO_4$ powders exhibit a photocatalytic activity in the degradation of MG under UV-light irradiation. The experimental milling conditions influence on the photocatalytic activity. The mechanochemical treatment may be used as an alternative route for the preparation of AWO_4 group oxides.

Acknowledgment

Thanks are due to the Financial Support of Bulgarian National Science Fund, Ministry of Education and Science Grants: TK-X-1702/07.

References

[1] A.W. Sleight, Acta Crystallogr. 28 (1972) 2899–2991.
[2] T.M. Yanushekevoch, V.M. Zhukovski, E.V. Tkachengo, Zh. Neorg. Khim. 33 (1978) 2485–2491.
[3] D.J. Morell, J.S. Cantreel, L.L.Y. Chang, J. Am. Ceram. Soc. 63 (1980) 261–264.
[4] P.F. Scholied, K.S. Knight, G. Cressey, J. Mater. Sci. 31 (1996) 2873–2878.
[5] T.O. Takagi, T. Fukuzawa, Appl. Phys. Lett. 36 (1980) 278–281.
[6] M. Bonanni, L. Spanhel, M. Lerch, E. Füglein, G. MüLler, Chem. Mater. 10 (1998) 304–310.
[7] Z. Lou, J. Hao, M. Covivera, J. Lumin. 99 (2002) 349–354.
[8] F.S. Wen, X. Zhao, H. Huo, J.-S. Chen, E. Shu-Lin, J.-H. Zhang, Mater. Lett. 55 (2002) 152–157.
[9] S.J. Chen, J.H. Zhou, X.T. Chen, J. Li, L.H. Li, J.M. Hong, Z. Xue, X.Z. You, Chem. Phys. Lett. 375 (2003) 185–190.
[10] D. Chen, G. Shen, K. Tang, H. Zheng, Y. Qian, Mater. Res. Bull. 38 (2003) 1783–1789.
[11] X. Jiang, J. Ma, J. Liu, Y. Ren, B. Lin, J. Tao, X. Zhu, Mater. Lett. 61 (2007) 4595–4598.
[12] M. Itoh, T. Katagiri, T. Aoki, M. Fujita, Rad. Meas. 42 (2007) 545–548.
[13] E. Cavalli, A. Belletti, M.G. Brik, J. Phys. Chem. Solids 69 (2008) 29–34.
[14] A. Kalinko, A. Kuzmin, J. Lumin. 129 (2009) 349–354.
[15] C. Ge, C. Xie, D. Zeng, S. Cai, J. Am. Ceram. Soc. 90 (2007) 3263–3267.
[16] X. Zhao, W. Yao, Y. Wu, S. Zhang, H. Yang, Y. Zhu, J. Solid State Chem. 179 (2006) 2562–2570.
[17] Y. Wu, S. Zhang, L. Zhang, Y. Zhu, Chem. Res. Chin. U 23 (2007) 465–468.
[18] G. Huang, Y. Zhu, Mater. Sci. Eng. B 139 (2007) 201–208.
[19] S. Lin, J. Chen, X. Weng, L. Yang, X. Chen, Mater. Res. Bull. 44 (2009) 1102–1105.
[20] H. Fu, J. Lin, L. Zhang, Y. Zhu, Appl. Catal. A: Gen. 306 (2006) 58–67.
[21] B. Liu, S.H. Yu, L. Li, F. Zhang, Q. Zhang, M. Yashimura, P. Shen, J. Phys. Chem. B 108 (2004) 2788–2792.
[22] G. Huang, Y. Zhu, J. Phys. Chem. C 111 (32) (2007) 11952–11958.
[23] H. Fu, C. Pan, L. Zhang, Y. Zhu, Mater. Res. Bull. 42 (2007) 696–706.
[24] G. Huang, H. Zhang, Y. Zhu, J. Alloys Compd. 432 (2007) 269–276.
[25] J. Lin, J. Lin, Y. Zhu, Inorg. Chem. 46 (2007) 8372–8378.
[26] G. Huang, S. Zhang, T. Xu, Y. Zhu, Environ. Sci. Technol. 42 (2008) 8516–8521.
[27] W. Zhao, X. Song, G. Chen, S. Sun, J. Mater. Sci. 44 (2009) 3082–3087.
[28] T. Dong, Z. Li, Z. Ding, L. Wu, X. Wang, X. Fu, Mater. Res. Bull. 43 (2008) 1694–1701.
[29] J. Bi, L. Wu, Z. Li, Z. Ding, X. Wang, X. Fu, J. Alloys Compd. 480 (2009) 684–688.
[30] C. Yu, J.C. Yu, Mater. Sci. Eng. B 164 (2009) 16–22.
[31] A.R. Phani, M. Passacantando, L. Lozzi, S. Santucci, J. Mater. Sci. 35 (2000) 4879–4883.
[32] J.H. Ryu, C.S. Lim, K.H. Auh, Mater. Lett. 57 (2003) 1550–1554.
[33] X. Jiang, J. Ma, J. Lin, Y. Ren, B. Lin, J. Tao, X. Zhu, Mater. Lett. 61 (2007) 4595–4598.
[34] P. Parhi, T.N. Karthik, V. Manivannan, J. Alloys Compd. 465 (2008) 380–386.
[35] R.C. Pullar, S. Farrah, N.McN. Alford, J. Eur. Ceram. Soc. 27 (2007) 1059–1063.
[36] A. Dodd, A. McKinely, T. Tsuzuki, M. Saunders, J. Eur. Ceram. Soc. 29 (2009) 139–144.
[37] J. Bystrzycki, T. Czujko, R.A. Varin, O. Oleszak, T. Durejko, W. darlewski, Z. Bojar, W. Przetakiewicz, Rev. Adv. Mater. Sci. 5 (2003) 450–454.
[38] V.V. Zyryanov, N.F. Uvarov, V.A. Sadykov, Y.V. Frolova, G.M. Alikina, A.I. Lukashevich, M.I. Ivanovskaya, J.M. Criado, S. Neophytides, Catal. Today 104 (2005) 114–119.
[39] Q. Zhang, F. Saito, J. Alloys Compd. 297 (2000) 99–103.
[40] H. Morimoto, M. Tatsumisaga, T. Minami, Electrochem. Solid-State Lett. 4 (2001) A16–18.
[41] I. Mitov, Z. Cherkezova-Zheleva, V. Mitrov, Phys. Status Solidi A 167 (1997) 475–479.
[42] S. Andonova, C. Vladov, B. Kunev, I. Mitov, G. Tyuliev, J.L.G. Fierro, S. Damyanova, L. Petrov, Appl. Catal. A: Gen. 298 (2006) 94–102.
[43] E. Avvakumov, M. Senna, N. Kosova, Soft Mechanochemical Synthesis: a Basis for New Chemical Technologies, Kluwer Academic Publishers, Boston, 2001.
[44] V.V. Zyryanov, Russ. Chem. Rev. 77 (2008) 107–137.
[45] V.V. Boldyrev, Russ. Chem. Rev. 75 (2006) 203–216.
[46] D. Klissurski, M. Mancheva, R. Iordanova, G. Tyuliev, B. Kunev, J. Alloys Compd. 422 (2006) 53–56.
[47] M. Mancheva, R. Iordanova, D. Klissurski, G. Tyuliev, B. Kunev, J. Phys. Chem. C 111 (2007) 1101–1104.
[48] W. Kraus, G. Nolze, PowderCell for Windows, Version 2.4, Federal Institute for Materials Research and Testing, Rudower Chanssee 5, (1996) 12489, Berlin, Germany.
[49] N.T. McDevitt, W.L. Baun, Spectrochim. Acta 20 (1964) 799–808.
[50] M.F. Daniel, B. Desbat, J.C. Lassegues, B. Gerand, M. Figlarz, J. Solid State Chem. 67 (1987) 235–247.
[51] C. Hariharan, Appl. Catal. A: Gen. 304 (2006) 55–61.
[52] Z. Yang, Q.H. Liu, Physica E 40 (2008) 531–535.
[53] M. Daturi, G. Busca, M.M. Borel, A. Leclaire, P. Piaggio, J. Phys. Chem. 101 (1997) 4358–4369.
[54] V.V. Fomichev, O.I. Kondratov, Spectrochem. Acta 50A (1994) 1113–1119.
[55] V. Šepelak, S. Indris, P. Heitjans, K.D. Becker, J. Alloys Compd. 434–435 (2007) 776–778.
[56] J. Yu, L. Qi, B. Cheng, X. Zhao, J. Hazard. Mater. 160 (2008) 621–628.